March, 2014. Vol. 4, No. 10 ISSN2305-8269
International Journal of Engineering and Applied Sciences

www.eaas-journal.org

THERMAL SENSING SYSTEM PREANALYSIS FOR A DIDACTIC ROCKET ENGINE BENCH

Annibal Hetem Junior, Lineu Ghaiasso Parra

Universidade Federal do ABC. Av. dos Estados, 5001. Bairro Bangu. Santo André - SP - Brasil

Abstract.

Due to operate at high temperatures and pressures, combustion chambers and nozzles thrusters present in rocket engines. These physical quantities are the main indicators of the behavior of the engine and are used to study its operation. The design of a rocket engine bench for educational purposes must establish a system for monitoring temperatures and pressures to allow better control and understanding of the processes occurring in this category of device. Data obtained from the engine is very important because the comparison between theory and practice is what makes knowledge to be learned deeply and with quality. This work presents studies of the placement of temperature sensors to be installed in specific positions of an ethanol fuelled rocket engine in order to monitor and study its operation.

Keywords: thermal sensing, thermocouple, supersonic nozzle, rocket engine.

1. INTRODUCTION

A main desired result from this work is to study the heat transfer and temperature and to propose sensors to be installed in specific positions of a rocket engine with ethanol in order to monitor and study its operation, providing data for future simulations and design enhancements.

As is well known, combustion reactions release large amounts of energy as heat. In a rocket engine, part of this energy is transferred to the walls of the combustion chamber and the nozzle. The regions where the temperature and heat transfer are more pronounced are specially relevant due to increased thermal stress components and can lead to catastrophic failure during operation (Sutton & Biblarz 2001). Moreover, the temperature and pressure are critical to the performance evaluation of the rocket motor during its test phase. These quantities can be used to estimate specific impulse and thrust that the engine is capable of achieve (Cornelisse et *al*. 1979).

This chapter intends to present our studies of a system for sensing heat and pressure of a rocket engine that uses liquid propellant (hydrogen peroxide and ethanol). In the designs of the proposed engine, the combustion chamber is preceded by a catalytic chamber where hydrogen peroxide is dissociated before reacting with ethanol. Fig. 1 shows the temperatures and pressures reached inside the nozzle from CFD simulations of our designed engine(Hetem et *al*. 2012).

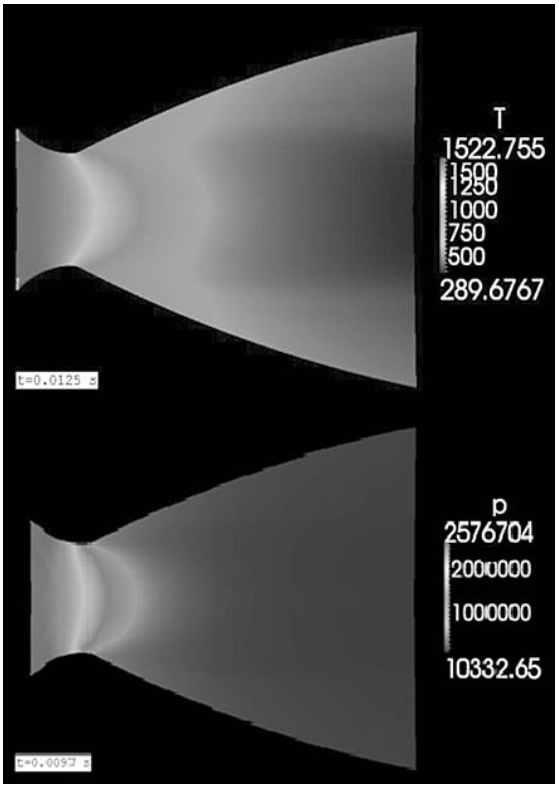

Figure 1. Results from simulations from Hetem et *al.* (2012) for the proposed engine temperatures (K) and pressure (Pa).

2. THE THERMAL MODEL

We consider as a preliminary thermal model an ideal rocket motor in order to explain what occurs in this type of equipment under simplified thermal processes. These considerations are:

a) At the entrance of the nozzle and inside of the combustion chamber, the physical characteristics of the gases are uniform;

b) The combustion and heat flow does not vary in time (steady state);

c) The combustion process is analyzed in detail and occurs in a small region within the combustion chamber;

d) The entry speed of the gases (mainly in the nozzle throat) is much smaller than its output speed;

e) The physical quantities are assumed constant in the surfaces normal to the streamlines.

It is also considered that the heat transfer due to its relevant importance in the project of an engine. Together with viscosity effects, these losses comprise 2% to 3% in total thrust produced (Cornelisse et *al.* 1979).

The combustion chamber is preceded by a catalytic chamber, in which the hydrogen peroxide separation occurs and results subsequently react with ethanol (Figure 2). Following Hetem et *al.* (2012), a combustion chamber with 1282.5 cm^3 shall be sufficient for proper burning of the propellant, and that will be necessary to install 24 injectors with 2 mm in diameter. The speed of injection of the propellant must be 19.04 m/s. Upon reaching the nozzle throat, the resulting gases are at $T_0 = 1461$ K under a pressure $p_0 = 25$ atm.

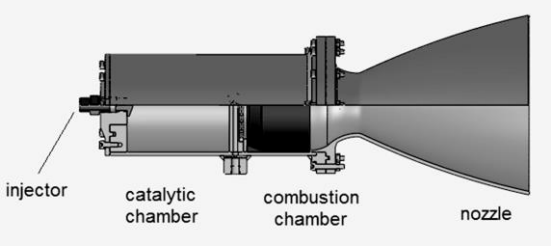

Figure 2. Details of the catalytic chamber and nozzle (Hetem et al. 2012)

One interesting characteristic of the project is the prevision that the walls of the combustion chamber and nozzle are covered by a layer of graphite. The walls themselves are made of stainless steel 0.5 cm thick. So, the thickness of the graphite should be sufficient to the temperature of the interface with the steel does not exceed the melting limit during the time interval of a typical launch.

There are a pair of heat transfer modes within the rocket motor: a) convective and b) radiative. The heat produced by the combustion is then transferred by conduction through the walls of the chamber and the nozzle and dissipated by convection and radiation to the environment in the outer surfaces. So, the engine in question is cooled exclusively by these radiative effects and natural convection due to the conditions that shall be present on the test bench. If needed, other cooling methods must be used in conjunction with the above to achieve a combined effect to ensure the safe operation of the engine. These extra methods are:

a) internal coating layer on the inner surface of a material with low thermal conductivity forming a thermal barrier on the inner side of the wall.

b) the use of film cooling in which a thin layer of fluid at a temperature lower than the buerned gases is maintained on the inner surface of the wall.

Following the formalism of convection and radiation as proposed by Cornelisse (1979), one considers the conservation equations of mass and moments, used in studies of fluid mechanics, and the law of Stefan-Boltzmann. The coefficient of convective heat transfer inside the combustion chamber can be expressed by equation (1) which was obtained from semi-empirical approach and is consistent with the experimentally observed results. It is us to establish the boundary conditions problem of heat transfer (Huzel & Huang 1971),

$$h_c = 0.026\left(\frac{\mu^{0.2} c_p}{\mathrm{Pr}^{0.6}}\right)\frac{\rho V^{0.8}}{D^{0.2}}\left(\frac{\rho_f}{\rho'}\right)\left(\frac{\mu_f}{\mu_0}\right) \qquad (1)$$

where h_c is the convective thermal coefficient of the gas, μ is the absolute gas viscosity, c_p is the specific heat of the gas at constant pressure, Pr is

the Prandt number, ρ is the mass density of the gas, V is the local gas velocity, D is the local chamber/nozzle diameter, ρ_f and μ_f refers to the density and viscosity at the arithmetic mean temperature of the local free-stream static temperature and the wall temperatures, ρ' is the free-stream value of the local gas density, and μ_0 refers to the viscosity evaluated at the stagnation or combustion temperature. Equation (2) represents the general case of transfer of heat by conduction in cylindrical coordinates with heat generation.

$$\frac{1}{r}\frac{\partial}{\partial r}\left(kr\frac{\partial T}{\partial r}\right)+\frac{1}{r^2}\frac{\partial}{\partial \theta}\left(k\frac{\partial T}{\partial \theta}\right)+\frac{\partial}{\partial z}\left(k\frac{\partial T}{\partial z}\right)+\dot{e}_{\text{gen}} = \rho c_p\frac{\partial T}{\partial t} \quad (2)$$

where r, θ and z are the cylindrical coordinates, t is time, is k is the conductivity of the gas, $\dot{e}_{\text{gen}}$ is the heat generation rate, and T is temperature. Considering cylindrical symmetry, steady state condition, and no generation of heat inside the wall of the chamber and the nozzle, equation (2) reduces to:

$$\frac{d}{dr}\left(r\frac{dT}{dr}\right)=0 \quad (3)$$

The simplified equation can be solved by ordinary integration. The boundary conditions are the temperature of the wall inside the combustion chamber (T_g) and the rates of heat transfer by conduction being equivalent to that by convection and radiation, because the contact interface with the gases does not store thermal energy. Thus,

$$q_r = -k\frac{\partial T}{\partial r} = h_c\left(T_g - T_w\right)+\varepsilon_g\sigma\left(T_g^4 - T_w^4\right) \quad (4)$$

where q_r is the heat transfer rate that leaves the internal surface, T_g is the temperature of the gas in contact with the wall, T_w is the temperature of the wall, ε_g is the radiative emissivity of the internal surface, and □ is the Stefan-Boltzmann constant. For convenience, the coefficients k and h_c can be considered constant at the first instance.

The temperature gradient occurs not only in the radial direction but also in the longitudinal axe, in the region of the nozzle. This means that the thermal diffusion differential equation should contains derivatives with respect to two spatial coordinates:

$$\frac{\partial}{\partial r}\left(r\frac{\partial T}{\partial r}\right)+\frac{\partial^2 T}{\partial z^2}=0 \quad (5)$$

For this kind of equation, only the cases where the geometry is simple can lead to formal exact solutions. For the more complex cases it is need to use computational methods, such as finite difference methods. Fig. 3 shows the adopted model of the thermal resistance of the wall of the combustion chamber. This model provides the total thermal resistance for the combustion chamber wall:

$$R_{\text{total}} = \left(\frac{1}{2\pi r_0 h_c L}+\frac{1}{2\pi r_0 h_{\text{R1}} L}\right)^{-1} + \frac{\ln(r_1/r_0)}{2\pi k_{\text{C}} L}+\frac{\ln(r_2/r_1)}{2\pi k_{\text{S}} L} + \left(\frac{1}{2\pi r_2 h_a L}+\frac{1}{2\pi r_2 h_{\text{R2}} L}\right)^{-1} \quad (6)$$

where r_0, r_1 and r_2 are the carbon layer internal radius, steel wall internal radius and chamber external radius respectively (see Fig 2), h_{R1} and h_{R2} are the thermal convective coefficients at positions r_1 and r_2, k_{C} and k_{S} are the conductive thermal coefficients of carbon and steel, h_a is the convective thermal coefficient of the air surrounding the engine, and L is the chamber length. As k_{C} and k_{S}, the thermal conductivities of graphite and steel, vary significantly with temperature, the values used in the model should be the average obtained in the temperature operating range of the engine (about 1600 °C).

March, 2014. Vol. 4, No. 10 ISSN2305-8269
International Journal of Engineering and Applied Sciences

www.eaas-journal.org

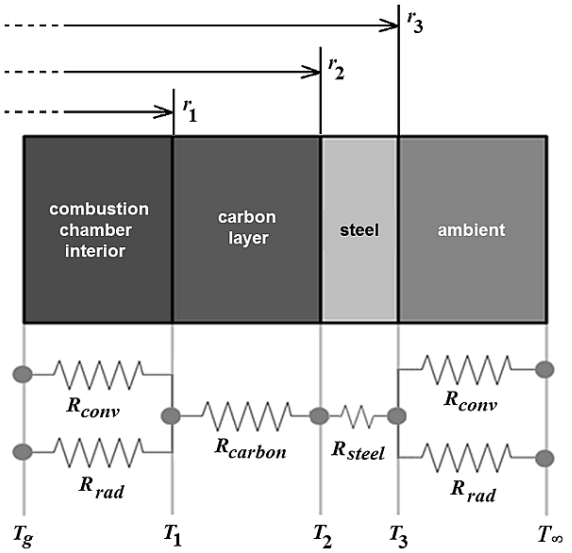

Figure 3. Thermal resistance model used to represent the heat transfer in the combustion chamber.

Approaching thermal conductivity as a linear function in the temperature range of operation of the engine, the k medium can be obtained by:

$$\bar{k} = \frac{1}{T_2 - T_1}\int_{T_1}^{T_2} k dT = k(\bar{T}) \qquad (7)$$

Three dimensionless numbers permit to evaluate heat losses by convection. The principal is the Grashof number (Gr) which is the equivalent of the Reynolds number for convection and represents the ratio between the thrust forces and viscous forces acting on the fluid. Also used are the Prandtl (Pr), Rayleigh (Ra) and Nusselt (Nu) numbers. The Nusselt number is regarded as a dimensionless coefficient of heat transfer by convection and represents the ratio between the rates of heat transfer by conduction and convection across the fluid layer. The Prandtl number is related to the relative thickness of the hydrodynamic and thermal boundary layers. For a horizontal cylinder, the Nusselt number can be estimated by (Çengel 2006):

$$\mathrm{Nu} = \left(0.6 + \frac{0.387\sqrt[6]{\mathrm{Ra}}}{\left[1+(0.059/\mathrm{Pr})^{9/16}\right]^{8/27}} \right)^2 \qquad (7)$$

with Ra = Gr × Pr and the Grashof number can be obtained by

$$\mathrm{Gr} = \frac{g\beta(T_s - T_\infty)L_C^3}{\nu^2} \qquad (8)$$

where g is the acceleration of gravitational, β is the coefficient of volume expansion (if one considers ideal gases, $\beta = 1/T$), T_s is the temperature of the surface, T_∞ is the temperature of the fluid sufficiently far from the surface, L_c is the characteristic length of the geometry, and ν is the kinematic viscosity of the fluid. Knowing these values, the convective coefficient will be given by

$$h = \frac{\mathrm{Nu}\, k}{L_c} \qquad (9)$$

Table 1 shows values of thermal conductivity (W/m K) at different temperatures for AISI 304 steel and the amorphous carbon. The properties k, Pr, β and ν are obtained for the temperature of the film equivalent to $T_f = (T_s+T_\infty)/2$.

Table 1. Thermal conductivity values of some materials (adapted from Çengel 2006).

Material	Thermal conductivity (W/m K)					
	100 K	200 K	400 K	600 K	800 K	1000 K
AISI 304 steel	-	-	16.6	19.8	22.6	25.4
Amorphous carbon	0.67	1.18	1.89	2.19	2.37	2.53

3. TEMPERATURE SENSORS

The thermocouple technology gives us a temperature-measuring device consisting of two dissimilar conductors that contact each other at one or more spots. It produces a voltage when the temperature of one of the spots differs from the reference temperature at other parts of the circuit. Thermocouples devices are able to operate in a wide temperature range, have a relatively low cost, can be used in environments with vibrations and there are also models that have fast response time. There are several commercial devices used to measure temperature, but the most suitable devices for the purposes of this project are in the thermocouples families.

A thermocouple is of simple construction, made by the junction of two wires made from different metals. This probe tip, often referred to as hot joint,

when subject to different temperatures responds with an electromotive force (emf).

This phenomenon is known as thermoelectric Seebeck effect, in honor of the physicist Thomas Johann Seebeck who first observed in 1821. Fixing one of the metals to a reference temperature, the other metal shall respond with a difference of potential (in volts). Then, one can write as a measure of the thermal sensitivity of the material, the Seebeck coefficient is defined as

$$\sigma(T) = \frac{dE_\sigma}{dT} \tag{10}$$

The liquid voltage difference can be obtained by performing the integration of the Seebeck coefficient between two extreme temperatures T_1 and T_2, or

$$E_\sigma = \int_{T_1}^{T_2} \sigma(T) dT \tag{11}$$

Table 2. Thermocouple types on the market and its most important characteristics (adapted from Williams 1998).

Thermocouple (designation / materials)	Seebeck coefficient (ΔV/°C)	Temp. range (°C)	e.m.f. produced (mV)
T / copper – constantan*	40.6	-270 800	25.0
J / iron - constantan	51.7	-270 1000	60.0
K / chromel** - alumel***	40.6	-270 1300	55.0
E / chromel - constantan	60.9	-270 1000	75.0
S / rhodium – platinum 10%	6.0	0 1550	16.0
R / rhodium – platinum 13%	6.0	0 1600	19.0

* Constantan is an alloy usually consisting of 55% Cu and 45% Ni.
** Chromel is an alloy of 90% Ni and 10% Cr.
*** Alumel is an alloy of 95% Ni and 5% Al.

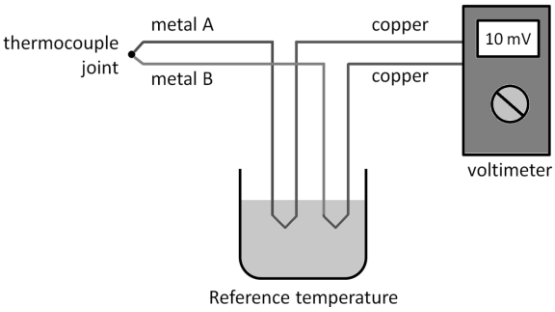

Figure 4. Example of a simplified system for measuring temperature used as a reference point ice water.

As it is not always easy to find an analytic function for this coefficient, in practice there are laboratory made tables that relate temperatures with tension produced for commercial thermocouples. Also, there are empirical polynomial expressions of degree less than or equal to nine which relate the approximate these two quantities.

Thermocouples available in the market have different formats, different junction metals. Some are projected to present low cost and others, more expensive, to provide rapid response time. If one chooses a thermocouple, it must be considered what the most appropriate for the desired application according to the characteristics of each type thermocouple, such as temperature range supported, the accuracy and reliability of the readings, among others. One should also take into consideration, in addition to specifying the type of alloy, the physical construction of the thermocouple. Table 2 shows the types of thermocouples on the market and their most important characteristics. Fig. 4 presents a construction of a simple system for measuring temperature using thermocouples.

The local temperature distribution can be significantly altered by thermocouples installed on surfaces. Thus, the temperature indicated by the measuring instrument (T_i) is the temperature due to the disturbance and not the actual surface temperature (T_s). The actual temperature can be found from a coefficient obtained experimentally or theoretically for each type of facility, known as factor installation (Z) which is expressed by $Z = (T_s - T_i)/(T_s - T_a)$ with T_a being the temperature of the surroundings or of the coolant.

A good mechanical support of the probe is required so that no stress or strain is applied to the

joint. In permanent installations on thin surfaces, the measuring junction of the thermocouple is attached directly to the surface, or mounted on a heat block. The joint can be welded, cemented or attached to the surface.

4. CONDITIONING AND DATA ACQUISITION

The order of the signals produced by a thermocouple is the range of milivolts. For reading these signals it is needed to be performed its amplification, what is done by an operational amplifier circuit. There is also the need of filters, responsible for the elimination of electromagnetic noise that may be introduced in the transmission of the signal from the sensor element to the data acquisition circuit.

The offset voltage output (V_{OS}) should be reduced in order to not introduce significant errors in measurement. The V_{OS} occurs due to an imbalance of the intrinsic circuit of the operational amplifier producing an output nonzero when both inputs are at 0 V. Sensors connected to the remote circuits require extensive differential amplifiers with high common-mode rejection ratio in order to eliminate part of the noise. The common-mode rejection ratio (CMRR), usually defined as the ratio between differential-mode gain and common-mode gain, indicates the ability of the amplifier to accurately cancel voltages that are common to both inputs. In devices that require high reliability in its measures, it should take into account the possibility of a ground terminal, and the wiring must be protected by an enclosure filters (Lepkowski 2004). Fig. 5 shows a circuit designed to amplify the signal from a thermocouple type K.

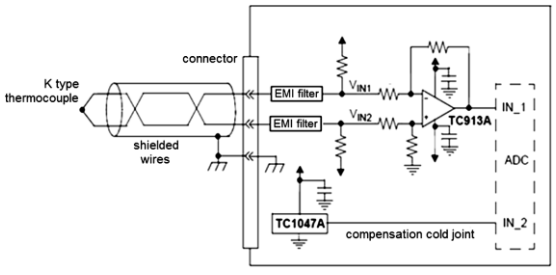

Figure 5. Circuit designed to amplify the signal from a thermocouple type K using a TC913A differential amplifier (Lepkowski 2004).

The reading of the sensors in our prototype is carried by a plate type development Arduino UNO R3. This board contains six analog inputs and an analog 10-bit digital. The analog inputs may operate with voltages at 0 volts and 5 volts which results in a resolution of about 4.9 mV. The time required to carry out the reading is 0.0001 enabling about 10,000 readings per second. Fig. 6 shows a temperature measuring system that provides both as signal conditioning, acquisition and data storage. Experimentally, we built a system control unit (with acquisition and data storage) with an Arduino processor.

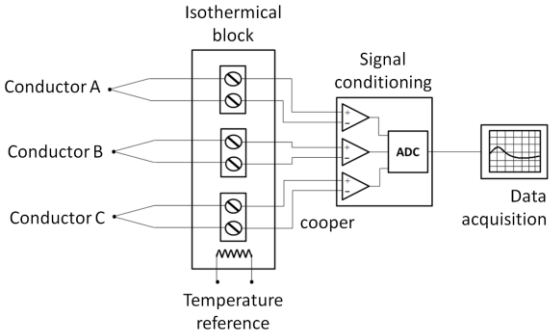

Figure 6. Block diagram of the data acquisition system.

5. RESULTS

As proposed by Çengel (2006), the convection coefficient has been calculated for various temperatures of the outer wall of the rocket engine. The temperature T_∞ considered was 25 °C and the temperature of the outer surface of the motor was measured to 1375 °C. The values of h are shown in the graph of Fig. 8. The average assumes the value of 8.9 W/m^2 °C. Similarly, k_S (average) = 21.0 W/m °C and k_C (average) = 1.6 W/m °C. The conditions inside the chamber are considered constant as well as its inner surface temperature, which is estimated in 1460 K. With a safety margin of 30%, one obtains a maximum temperature of about 1900 K which exceeds the melting point of the AISI 304 steel. So, the need for a graphite layer is real.

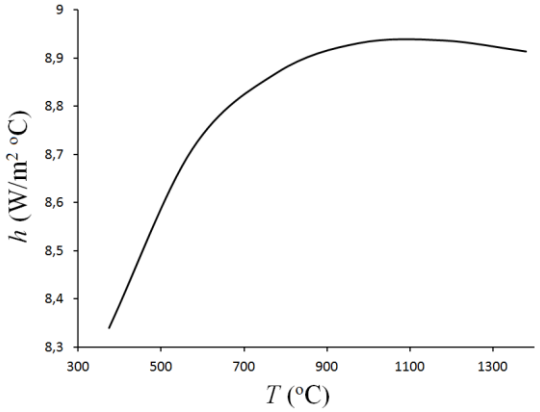

Figure 8. Model behaviour for the convective coefficient for the external engine surface.

The graphite layer thickness can be optimized so that the temperature at the interface graphite/steel does not reach the melting point of 1670 K. In the models, we assumed emissivity of the stainless steel business falls between 0.17 and 0.3. The total thermal resistance can be calculated, and the thickness of the graphite layer being presented with between 5 and 17 mm.

6. CONCLUSIONS

We presented the preliminary results of studies of heat transfer and temperature sensors to be installed in a rocket engine in order to monitor and study its operation, providing data for future simulations and design enhancements. We presented the thermal model and expressions to first order of heat transfer; some study on temperature sensors, with emphasis on bimetallic thermocouples; the conditions and data acquisition circuits, with construction of a experimental module.

The continuity of this project involves the use of more sophisticated techniques based on genetic algorithms for optimizing the thickness of the graphite layer and other thermal properties of the motor. The study the influence of the presence of fins on the radiative diffusion of external heat is also considered.

An important result for the continuity of this project is the estimation of convective coefficient between the rocket motor and the environment, which allowed the estimative of the protective carbon layer to be inserted in the combustion chamber.

7. ACKNOWLEDGEMENTS

The authors want to thank the Research Group of Liquid Propellant Rocket of UFABC (http://posmec.ufabc.edu.br/gpmfpl) for supporting this research. L.G.P. thanks the Provost of Research of Universidade Federal do ABC for general support.

8. REFERENCES

1. Çengel, Y. A.. Transferência de calor e massa: uma abordagem prática. 3ª edição. São Paulo: McGraw-Hill, 2009.
2. Cornelisse, J.W., Schoyer, H.F.R., Swakker, K.F., Rocket Propulsion and Space Flight Dynamics, Pitman, 1979.
3. Hetem, A.; Rafael, C. F.; Miraglia, J. . Simulation of supersonic catalytic green propellant nozzle rocket engine. Journal of Aerospace Engineering, Sciences and Applications, v. IV, p. 112-122, 2012.
4. Huzel, D., & Huang, D.H., Design of Liquid Propellant Rocket Engines, NASA SP-125, National Aeronautics and Space Admnistration, 1971.
5. Lepkowski, J., Temperature Measurement Circuits for Embedded Applications, Microchip Technology Inc., 2004.
6. Sutton, G.P., & Biblarz, Rocket Propulsion Elements, John Wiley & Sons, 2001.
7. Williams, J., Application Note 28: Thermocouple Measurement, Linear Technology. 1998.